NeuroImage 197 (2019) 255–263

Contents lists available at ScienceDirect

NeuroImage

journal homepage: www.elsevier.com/locate/neuroimage

Enhanced high-frequency precuneus-cortical effective connectivity is associated with decreased sensory gating following total sleep deprivation

Liwei Zhang [a,b,c], Yue Huang [d], Ying Zhang [e], Wei Xin [f], Yongcong Shao [a,*], Yebing Yang [f,**]

[a] Department of Psychology, Beijing Sport University, Beijing, 100084, China
[b] School of Biological Science and Medical Engineering, Beihang University, Beijing, 100083, China
[c] Beijing Advanced Innovation Centre for Biomedical Engineering, Beihang University, Beijing, 102402, China
[d] Department of Medical Psychology, Army Medical University, Chongqing, 400038, China
[e] The Eighth Medical Center, The General Hospital of the People's Liberation Army, Beijing, 100091, China
[f] The Sixth Medical Center, The General Hospital of the People's Liberation Army, Beijing, 100048, China

ARTICLE INFO

Keywords:
Sleep deprivation
Sensory gating function
Electroencephalogram
Effective connectivity

ABSTRACT

Sleep deprivation decreases an individual's cognitive function. When cognitive impairment reaches a certain level, human errors occur and may even result in accidents. Previous research has shown that sensory gating is a basic mechanism in cognitive function, but only limited studies have so far reported how it is affected by sleep deprivation. This study aimed to analyze the effects of sleep deprivation on sensory gating and its cognitive and neural mechanisms. Thirty-six healthy subjects participated in our study. The resting-state, auditory P50-task electroencephalography (EEG) recordings and the psychomotor vigilance task (PVT) were performed at resting wakefulness (RW) and after 36 h of total sleep deprivation (TSD). Changes in P50 suppression before and after sleep deprivation were recorded, and the isolated effective coherence (iCoh) was employed for analyzing effective connectivity based on EEG data during the resting-state and P50 tasks. Subjects demonstrated reduced P50 suppression and prolonged PVT reaction time after TSD compared with RW. Effective connectivity analysis of resting-state EEG data showed that sleep deprivation decreased the connectivity from the right middle occipital gyrus (RMOG)/Rcuneus to left inferior/middle temporal gyrus (LITG/LMTG) and left parahippocampal/fusiform gyrus (LPH/LFG). EEG data analysis during the P50 task showed that, in addition to the aforementioned connectivity changes, the directed high-frequency effective connectivity from the left precuneus to the left superior/middle frontal gyrus (LSFG/LMFG), LITG/LMTG, LPH/LFG, and left middle occipital gyrus (LMOG)/Lcuneus increased. P50 suppression in Cz positively correlated with PVT reaction time. This study reveals that the precuneus is a key brain region in neural network correlates of sensory gating, and that changes in its effective connectivity with other regions (including LSFG/LMFG, LPH/LFG, LMOG/LCuneus, and LITG/LMTG) are important for decreasing sensory gating after TSD.

1. Introduction

Sensory gating is a basic cognitive function, mainly characterized by reduced evoked responses to repeated stimulation (Boutros and Belger, 1999; Freedman et al., 1996; Ringel et al., 2004). This automatic mechanism can protect higher-level cognitive networks from sensory information overload (Adler et al., 1982; Freedman et al., 1983). It constitutes a fundamental cognitive mechanism for attention and is important for memory, reasoning, and other higher cognitive functions, as it enables an individual to focus his/her attention on oddball stimuli, thereby saving attention resources (Morales-Muñoz et al., 2016).

The most common measuring methods for sensory gating include the two event-related potentials (ERPs) in electroencephalography (EEG): P50 (Bramon et al., 2004; Clementz et al., 1997; Nagamoto et al., 1989)

Abbreviations: EEG, electroencephalography; RW, resting wakefulness; TSD, total sleep deprivation; iCoh, isolated effective coherence; MOG, middle occipital gyrus; ITG/MTG, inferior/middle temporal gyrus; PH/FG, parahippocampal/fusiform gyrus; SFG/MFG, superior/middle frontal gyrus; ERPs, event-related potentials; PPI, prepulse inhibition; EOG, electrooculogram; eLORETA, low-resolution electromagnetic tomography.

* Corresponding author. No 48, Xinxi Road, Haidian District, Beijing, China.
** Corresponding author. No. 6 Fucheng Road, Haidian District, Beijing, China.
E-mail addresses: budeshao@aliyun.com (Y. Shao), yangyebing2005@aliyun.com (Y. Yang).

https://doi.org/10.1016/j.neuroimage.2019.04.057
Received 16 January 2019; Received in revised form 13 April 2019; Accepted 20 April 2019
Available online 25 April 2019

and prepulse inhibition (PPI) (Petrovsky, 2014). P50 suppression is measured during the period when two identical auditory stimuli are presented. Sensory gating is defined as the reduction in ERP amplitude between the P50 produced by the first and that produced by the second stimulus (Anokhin et al., 2007). Hamilton et al. (2018) found that P50 is closely associated with working memory and the speed of information processing, which are often measured by the psychomotor vigilance task (PVT) (Price et al., 2017). PPI is calculated as the percentage decrement in the startle amplitude in the presence versus absence of a prepulse stimulus, i.e., 100 − [prepulse amplitude/pulse amplitude]*100 (Morales-Muñoz et al., 2016). Functional magnetic resonance imaging studies have shown that brain regions associated with sensory gating are mainly concentrated in the frontal, temporal, and occipital lobes (Bak et al., 2011; Mayer et al., 2009).

Sleep deprivation is a phenomenon that many modern people experience. Many studies have shown that sleep deprivation causes a significant decline in cognitive function, including deficits in attention, working memory, and decision-making (Choo et al., 2005; Havekes et al., 2016; Lim and Dinges, 2010). Moreover, sleep deprivation significantly reduces the N2 and P3 amplitudes of ERPs but increases their latencies, suggesting significant impairments in the brain's alerting function (Cote et al., 2008; Jin et al., 2015). Recently, a study demonstrated that one night of sleep deprivation leads to decreased effective connectivity from the posterior to the anterior cingulate gyrus, indicating that sleep deprivation disrupts this directed information flow (Piantoni et al., 2013). In addition, sleep deprivation also causes significant changes in brain network connectivity (Verweij et al., 2014).

Sleep deprivation reduces sensory gating, which is important for filtering out irrelevant information, rationally distributing cognitive resources, and basic cognitive functioning (Monica et al., 2006). Many studies have shown that P50 occurs before attention, is not affected by attention regulation (Braff and Light, 2004; Boutros et al., 2004; Jerger et al., 1992), and is the basis of alerting function. Several studies have shown that sensory gating deficits due to sleep deprivation are similar to those of schizophrenia (de Gelder et al., 2003; Petrovsky et al., 2014; Ross et al., 2007). In schizophrenia, researchers found that the temporal and prefrontal lobes were connected intimately with sensory gating functions (Tregellas et al., 2007). This suggests that changes in network connectivity are intimately associated with impairments in behavioral responses. Although sensory gating is significantly impaired by PPI after sleep deprivation (Petrovsky et al., 2014; Gumenyuk et al., 2013), only one study has explored P50 suppression changes and found that it decreases after TSD, compared with RW (Wu et al., 2013).

An essential characteristic of the healthy brain is the efficient communication between distant cortical areas, which is necessary for proper cognitive functioning (Deco and Corbetta, 2011; Deco et al., 2011). Functional connectivity indicates the long-distance communication by depicting the degree of correlation between region-specific activity (Deco et al., 2011). Converging evidence indicates that functional connectivity fluctuations have neurobehavioral significance (Chang et al., 2016; Rosenberg et al., 2016), particularly in relation to shifts in attention or arousal, including falling asleep (Chang et al., 2016; Wang et al., 2016). In the past, EEG could not reflect the functional connectivity among brain regions, thus making cognitive and neural mechanisms hard to explain. In recent years, functional connectivity methods, such as Granger causality, orthogonalized partial directed coherence, dynamic causal modeling, and isolated effective coherence (iCoh) have attracted the attention of several researchers. Currently, iCoh is the main method used for analyzing spectral information of effective connectivity, as it allows the in-depth analysis of the directionality of effective connectivity among brain regions of interest, assessment of whether connectivity is direct or indirect, and investigation of its spectral characteristics (Pascual-Marqui et al., 2014a).

In this study, we employed iCoh to analyze changes in effective connectivity among brain regions associated with sensory gating before and after sleep deprivation, in order to examine the neural mechanisms of sensory gating deficits after sleep deprivation. We hypothesized that (1) sleep deprivation would result in reduced sensory gating, which would be correlated with the decreased RT of the PVT task; and (2) that a significant decrease in effective connectivity associated with sensory gating would occur after sleep deprivation. We recorded resting-state and P50 task EEGs under resting wakefulness (RW) and after 36 h of total sleep deprivation (TSD) and compared the changes in P50 marker.

2. Materials and methods

2.1. Subjects

Thirty-six healthy male adult volunteers participated in the current study. All subjects (age range 22–29 years, mean age = 25 ± 3.5 years) were right-handed, had a normal or corrected-to-normal vision, and normal hearing. A doctor confirmed that subjects had no psychiatric disorder. They all had good sleeping habits, slept 7–9 h a day, and no subject reported a history of insomnia.

This study was conducted according to the principles of the 1964 Declaration of Helsinki and obtained approval by the ethics committee of the Beihang University and Chinese People's Liberation Army Naval General Hospital. Before formal testing, subjects fully understood the test's content and rules and provided written informed consent. All subjects were given a monetary ($510) reward after the test.

2.2. PVT

We chose the PVT to test subjects' alertness level. Red dots (diameter = 3 cm, viewing angle 1.5 × 1.5°) were displayed in the center of a white background on an LCD screen (1024 × 768; refresh rate 60 Hz). At the beginning of each trial, subjects looked at the '+' focus in the center of the screen for 400 ms. After that, the red dots appeared in the center of the screen, and the red dot disappeared immediately after the subject responded. The red dots lasted for 1000 ms at most. The interval between trials was 8–12 s (mean = 10 s, pseudo-random change of stimulus interval). Subjects were asked to respond as soon as possible after the stimulus appeared, but no early response was allowed. Participants completed 30 trials of the PVT. When the RT was ≥ 100 ms, a response was defined as a valid PVT response. Errors included false alarm (RT < 100 ms), lapses (≥1000 ms), and pressing the wrong button.

2.3. Resting-state and P50-task EEG

The experiments were conducted in a sound-proof and electromagnetically shielded room. The subject was seated comfortably in the room. First, a 3-min resting-state EEG acquisition task was completed under a resting wakeful state. During the acquisition process, the subject was asked to keep his eyes open. Next, the subject completed the P50 task, while EEG was recorded. The P50 task was carried out using foam-tipped earphones that presented auditory stimuli. The subject passively listened to a pair of pure-tone stimuli, which were recorded as stimulus 1 (S1) and S2, with both ears. The two stimuli lasted for 5 ms, with an inter-stimulus interval of 500 ms, a sound pressure level of 80 dB, and a frequency of 500 Hz. During the experiment, subjects were not required to respond to the auditory stimuli. Each trial comprised of a pair of auditory stimuli, and the P50 task comprised 30 trials. The interval between S2 and S1 of the next trial was 10 s. A visual fixation cross "+" (visual angle = 2.8°) was present during the entire experimental process, to minimize eye movements.

2.4. EEG recording

EEG data were recorded during the resting-state and P50 tasks. EEG acquisition was carried out using the 10–20 standard system. The 32-channel Quik-Cap was used for continuous recording of EEG data. The SynAmps2 amplifier (Neuroscan Products), including a 0.01–100-Hz

band filter and 50-Hz notch filter, was used for sampling at 1000 Hz. The impedance was kept below 5 kΩ for all electrodes during the experiment. A bilateral mastoid was used as a reference electrode. Horizontal electrooculogram (EOG) was recorded at the outer corner of the eyes and vertical EOG at the upper and lower corner of the right eye.

2.5. Procedure

On the day before the test, the subjects completed a hearing test to verify that their hearing was within the normal range. Subjects who passed the test were informed of the experimental content and rules. Then, subjects were instructed to obtain approximately 8 h of sleep. At the beginning of the formal experiment, at 8:00 in the morning, subjects completed the two tasks (resting state and P50) in an order. Thirty-six hours after the initial testing, subjects repeated the two tasks in the same order (Fig. 1). Importantly, over the 36-h period between the first and second test, subjects were monitored continuously and were not allowed to sleep. During the experiment, subjects were always accompanied by the experimenters, who made sure the subject did not fall asleep during the sleep deprivation paradigm by using an inquiry before and a retrospective verbal report after each session. Subjects were only allowed to perform nonstrenuous activities, such as conversing, reading, and working on a computer. Moreover, subjects were not permitted to smoke, or drink coffee, chocolate, and alcohol.

2.6. Data analysis

2.6.1. EEG and ERP data processing

The raw EEG data of the resting-state and P50 tasks were analyzed offline using Scan 4.5 (Neuroscan Products). The reference electrode was converted from a bilateral mastoid to a common average reference. Next, eye movement artifacts in the EEG were corrected using time-domain regression analysis (Kenemans et al., 1991). Artifacts in electromyogram were rejected using a voltage monitor, with parameters set to block intervals ranging from −100 ms, pre-artifact, to 100 ms, post-artifact, and the amplitude set between −100 and 100 μV. After raw data artifact reduction, a 0.5–40-Hz band-pass filter was used to filter the data. The frequency slope of the filter was 24 dB/oct. EEG data from six subjects were excluded from further analysis due to an insufficient number of acceptable trials on the 36-h TSD, after excluding trials contaminated with EEG artifacts.

For the P50 task, stimuli-locked epochs with a length of 500 ms, including 100 ms before the onset of the stimuli, were used. Stimuli-locked amplitude averages were computed separately for each participant and each auditory stimulus. Then, stimuli-locked ERPs were baseline corrected for the interval of −100 to 0 ms prior to the stimuli. The ERP-component P50 was defined as the max positive peak occurring at 30–100 ms after the stimulus. P50 peaks were extracted at channel Cz.

2.6.2. Effective connectivity extraction

As scalp signals themselves cannot be used to study cortical connections, we used low-resolution electromagnetic tomography (eLORETA) (Pascual -Marqui, 2007; Pascual-Marqui et al., 2011) to generate estimated cortical signals, to calculate the strength of connections. We chose eLORETA, because it can accurately estimate neuronal current density, effectively reduce the effects of volume conduction, and is verified by many experiments (Pascual-Marqui et al., 2014b). It has been shown that eLORETA is an effective tool for functional mapping, because it is consistent with physiology, can provide correct locations (Pascual--Marqui, 2002), and reproduces the independent verification of localization properties (Wagner et al., 2004). In addition, previous studies have shown that eLORETA can be used to precisely locate deep brain structures, such as the subgenual anterior cingulate cortex (Pizzagalli et al., 2004) and medial temporal lobe (Zumsteg et al., 2006a, b, Pascual-Marqui et al., 2014b, Ridder et al., 2015). Another study showed that despite the small number of electrodes (e.g., 19) that are used in eLORETA to estimate signals and the relatively high levels of biological and measurement noise damage, from a qualitative point of view, good results can still be obtained (Pascual-Marqui et al., 2014b). Following that, we employed iCoh to quantify the intensity and direction of effective connectivity (Pascual-Marqui et al., 2014a), as an effective measure to correctly assess direct connections that causally transmit oscillatory information between nodes, under the assumption of a multivariate autoregressive model. iCoh was calculated by formula (1).

$$k_{i\leftarrow j}(\omega) = \frac{[s_\varepsilon]_{ii}^{-1}\left|[A(\omega)]_{ij}\right|^2}{[s_\varepsilon]_{ii}^{-1}\left|[A(\omega)]_{ij}\right|^2 + [s_\varepsilon]_{jj}^{-1}\left|[A(\omega)]_{jj}\right|^2} \quad (1)$$

where, ω is the frequency, which is 0,1 …$N_T - 1$; $k_{i\leftarrow j}(\omega)$ is the iCoh value from the jth to the ith brain region (range of 0–1); $A(\omega)]A(\omega)]_{ij}$ is the discrete Fourier transform matrix with a causal relationship with regions j and i; and s_ε is the covariance matrix.

In both RW and TSD conditions, the same estimated multivariate autoregressive model of $p = 7$ order was used to estimate iCoh values for the regions of interest.

We confirmed the cortical points associated with sensory gating by referring to brain regions associated with the P50 sensory gating function (Mayer et al., 2009) (Table 1). The electrical activity from eight cortical points was entered into the forward equation that was solved using EEG signals from 30 cortical electrodes. In order to calculate iCoh, EEG data were loaded into an inverse solver (i.e. the solution space composed of 6239 cortical gray matter voxels at 5-mm spatial resolution in eLORETA) to generate estimated cortical signals. iCoh analysis was further conducted using the following six frequency segments: delta (0.5–4 Hz), theta (4–7 Hz), alpha (8–13 Hz), beta1 (14–20 Hz), beta2 (20–30 Hz), and gamma (30–40 Hz).

2.6.3. Statistical analyses

Before and after sleep deprivation, we computed (TSD - RW) the PVT reaction time, P50 suppression (S1-S2 amplitude), and connectivity strength suppression (S1 (iCoh)-S2 (iCoh)) and used paired t-tests to compare the differences between conditions (RW and TSD). The number of errors on the PVT task, before and after TSD, were compared using the Wilcoxon test. Differences were considered significant at a probability of 0.05. We calculated the differences among P50-iCoh values before and

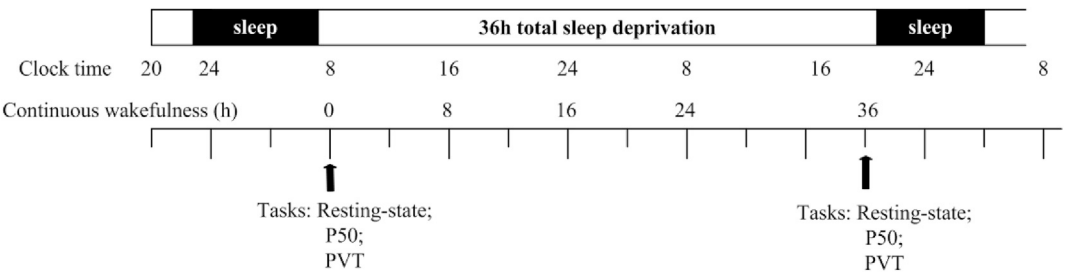

Fig. 1. Study protocol. Subjects underwent a 36-h period of total sleep deprivation. The black arrows indicate the time points of the resting-state and P50 tasks.

Table 1
Talairach coordinates of the centroid voxel for the frontal, temporal, parietal, and occipital.

Regions of interest	Structure	Brodmann area	Side	*X*	*Y*	*Z*
Frontal lobe	Superior and middle frontal gyrus	10/11	R	22	52	−10
Frontal lobe	Superior and middle frontal gyrus	9/46	L	−39	37	26
Temporal lobe	Inferior and middle temporal gyrus	37	L	−50	−63	5
Temporal lobe	Parahippocampal and fusiform gyrus	19/37	L	−26	−50	−8
Temporal lobe	Parahippocampal and fusiform gyrus	19/37	R	29	−53	−3
Parietal lobe	Precuneus	7	L	−25	−45	41
Occipital lobe	Middle occipital gyrus, cuneus	18/37	L	−28	−85	13
Occipital lobe	Middle occipital gyrus, cuneus	18/37	R	29	−80	11

NOTE: Side refers to the hemisphere showing activation, where L = left, and R = right hemisphere. X, Y, Z refer to Talairach coordinates from the center of mass.

after TSD. For connectivity analyses, we employed the multiple-comparisons correction procedure implemented in the LORETA statistical package, a nonparametric permutation test based on voxel intensity (Nichols and Holmes, 2001). We also performed Pearson correlation analysis of changes in PVT reaction time and P50 suppression, before and after TSD.

Table 2
Changes in PVT parameters (mean ± SEM).

	RW	TSD	T(Z)	P
RT (ms)	333.84 ± 6.27	383.66 ± 9.54	7.685	<0.001
Number of Errors	0.27 ± 0.17	0.77 ± 0.22	2.054	0.04

NOTE: PVT, psychomotor vigilance task; RW, resting wakefulness; TSD, total sleep deprivation; RT, reaction time; SEM, Standard Error of Mean.

3. Results

3.1. PVT reaction time

There was significant difference in PVT reaction time and number of errors between RW and TSD ($t = 7.685$, $p < 0.001$; Table 2).

3.2. ERP-component P50 amplitude

The results for the grand average ERP waveforms for each condition are shown in Fig. 2. P50 mean amplitudes and suppression differences are presented in Table 3. P50 suppression was lower after TSD compared with RW ($t = 2.793$, $p = 0.019$; Table 3). P50 amplitude in response to S1 showed no difference between the two conditions ($t = 0.53$, $p = 0.606$). Although the magnitude of the S2 amplitude response was larger after TSD compared with RW, the difference was not statistically significant ($p = 0.25$).

3.3. Effective connectivity during the P50 task

Statistical comparison of iCoh values of connectivity strength suppression between the RW and TSD conditions was carried out for each pair of regions of interest and for each connectivity direction. The grand averages for the connectivity strength suppression for each condition are shown in Fig. 3. Fig. 4 summarizes the main statistically significant results. In high frequency bands, we obtained significant results for the connection from the precuneus to several regions, including the left

Table 3
P50 amplitude in channel Cz obtained under resting wakefulness (RW) or total sleep deprivation (TSD).

	RWMean (SEM)	TSDMean (SEM)	T (paired *t*-test)	P (paired *t*-test)
S1	1.25 (0.18)	1.08 (0.27)	0.530	0.606
S2	1.12 (0.38)	1.83 (0.6)	−1.187	0.250
S1-S2	1.63 (0.33)	−0.59 (0.79)	2.793	0.019*

NOTE: *, P < 0.05. SEM, Standard Error of Mean; S, stimulus.

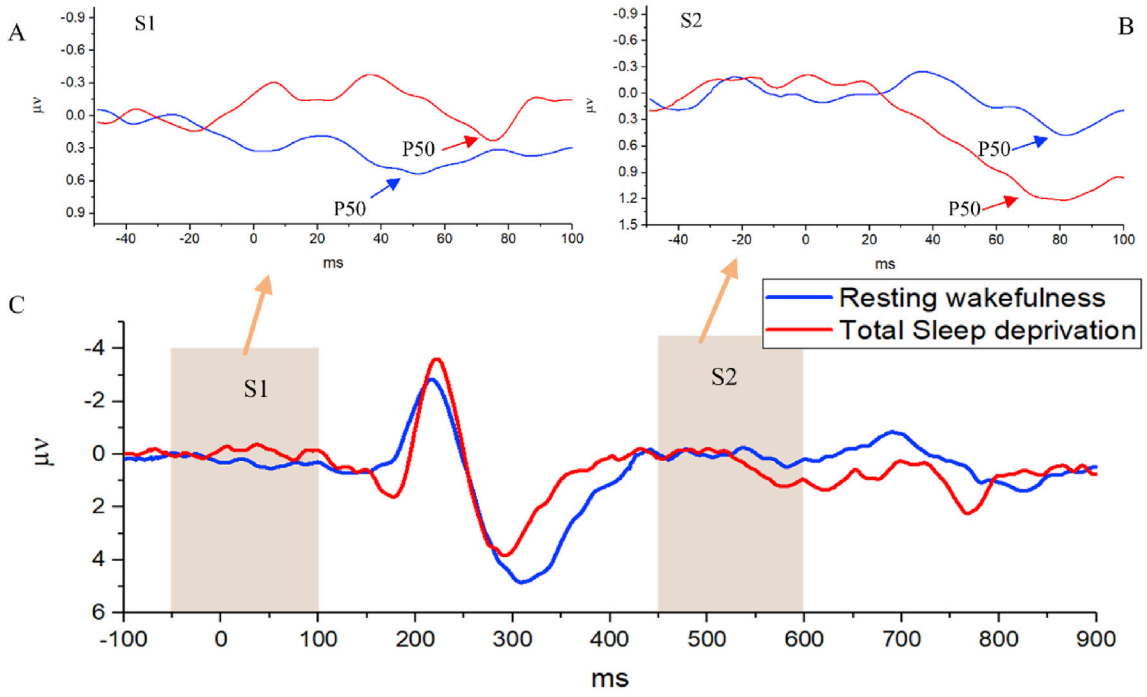

Fig. 2. A. Grand average of P50 waveforms corresponding to S1 and S2 obtained under resting wakefulness (blue line) or total sleep deprivation (red line). B. Grand average of S1-P50 waveforms. C. Grand average of S2-P50 waveforms.

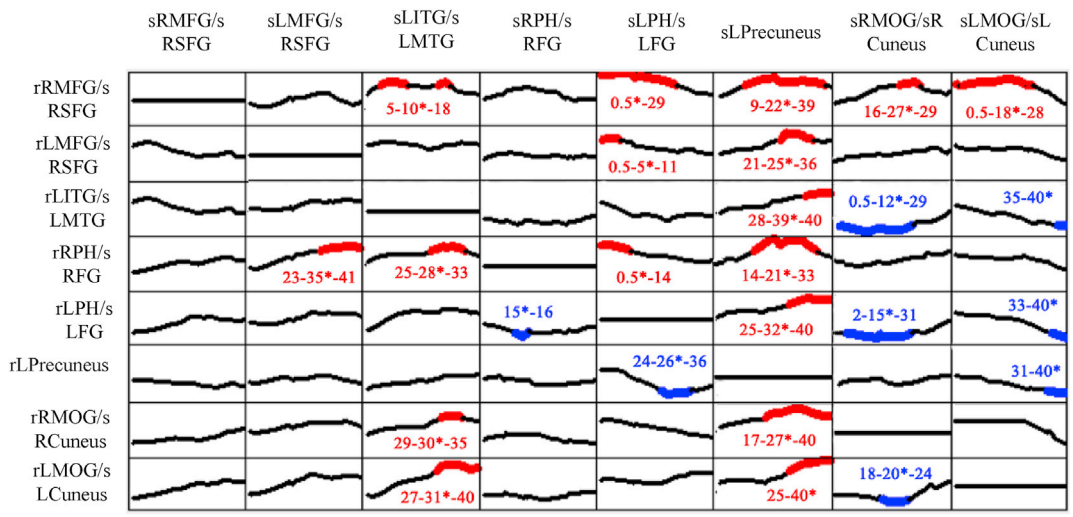

Fig. 3. Paired t-statistics comparing isolated effective coherence (iCoh) values after total sleep deprivation (TSD) and at resting wakefulness in the P50 task, in eight regions of interest: left superior and middle frontal gyrus (LSFG/LMFG), right superior and middle frontal gyrus (RSFG/RMFG), left inferior and middle temporal gyrus (LITG/LMTG), left parahippocampal and fusiform gyrus (LPH/LFG), right parahippocampal and fusiform gyrus (RPH/RFG), left precuneus (LPrecuneus), left middle occipital gyrus and cuneus (LMOG/LCuneus), and right middle occipital gyrus and cuneus (RMOG/RCuneus). Frequency axis: 0.5–40 Hz. Corrected $p = 0.05$ at t-threshold = 2; vertical axis, −3.5 to +3.5. Blue color denotes significantly stronger suppression of the connectivity strength during RW compared with TSD; red color denotes significantly stronger suppression after TSD compared with RW. The three numbers in the figure represent the frequency (Hz) where significant results were obtained: the beginning, the most significant oscillation represented by the superscript "*", and the end. Columns are "sender" regions (prefix "s"), and rows are "receiver" regions (prefix "r").

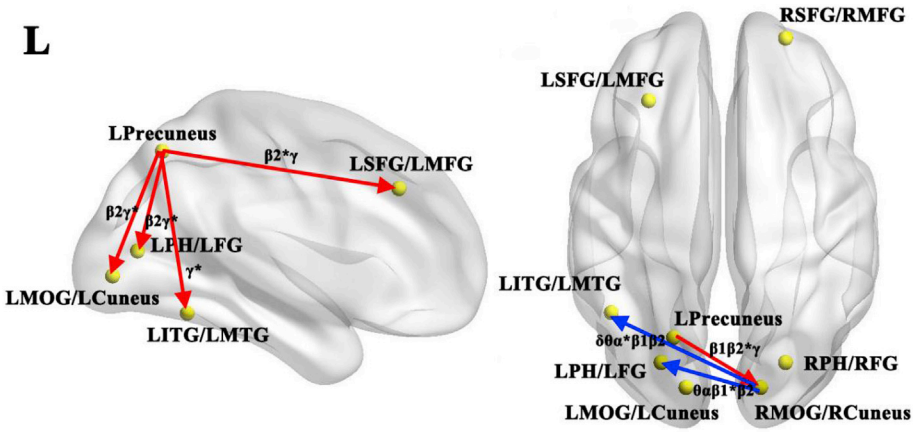

Fig. 4. Network properties comparison between resting wakefulness and total sleep deprivation (TSD) in the P50 task. Summary of the main statistically significant results. Blue color denotes significantly stronger suppression of the connectivity strength during RW compared with TSD; red color denotes significantly stronger suppression after TSD compared with RW. High-frequency oscillations are sent from the left precuneus to several regions, including the left superior and middle frontal gyrus (LSFG/LMFG), left parahippocampal and fusiform gyrus (LPH/LFG), left middle occipital gyrus and cuneus (LMOG/LCuneus), and left inferior and middle temporal gyrus (LITG/LMTG). right superior and middle frontal gyrus (RSFG/RMFG); right parahippocampal and fusiform gyrus (RPH/RFG); right middle occipital gyrus and cuneus (RMOG/RCuneus). Frequency bands: δ, 0.5–4 Hz; θ, 4–7 Hz; α, 8–13 Hz; β1, 14–20 Hz; β2, 20–30 Hz; γ, 30–40 Hz.

superior and middle frontal gyrus (LSFG/LMFG), left parahippocampal and fusiform gyrus (LPH/LFG), left middle occipital gyrus and cuneus (LMOG/LCuneus), and left inferior and middle temporal gyrus (LITG/LMTG).

3.4. Correlations between changes in cortical connectivity and changes in sensory gating

Table 4 shows the correlations between changes in cortical connectivity and changes in sensory gating (see the last page). Changes in effective connectivity from the LPC to the LSFG/LMFG, LPH/LFG, LMOG/LCuneus, LITG/LMTG, and RMOG/RCuneus, and from the RMOG/RCuneus to the LITG/LMTG and LPH/LFG significantly correlated with changes in the SG in many channels, and frequency bands. All significant correlations between changes in effective connectivity from the LPC to the LPH/LFG, LMOG/LCuneus, LITG/LMTG, and RMOG/RCuneus significantly negatively correlated with changes in the SG on the gamma band.

3.5. Effective connectivity during the resting-state task

Fig. 5 shows the connections among the eight brain regions of interest at 0.5–40 Hz. Fig. 6 shows a schematic summary of the main statistically significant results. In the low-frequency band, the connections from the right MOG/cuneus (RMOG/RCuneous) to the LITG/LMTG and LPH/LFG, as well as the connection from the LPH/LFG to the RMOG/RCuneus were statistically significant.

3.6. Correlation between changes in P50 suppression and in PVT reaction time

The results from the Pearson correlation analysis between changes in P50 measures and PVT performance are presented in Fig. 7 ($r = 0.618$, $p = 0.004$).

4. Discussion

In this study, we analyzed and compared changes in auditory ERP-

Table 4
Correlation between changes in cortical connectivity and changes in SG.

Connectivity	Delta		Theta		Alpha		Beta1		Beta2		Gamma	
	channel	*r(p)*	channel	*r(p)*	channel	*r(p)*	channel	*r(p)*	channel	r(p)	channel	*r(p)*
LPC→LSFG/LMFG									P3	0.387 (0.034)		
LPC→LPH/LFG	P7	0.606 (0.000)	F7	−0.365 (0.048)	F7	−0.391 (0.033)	T8	−0.444 (0.014)	F8	−0.458 (0.011)	T7	−0.409 (0.025)
	P3	0.452 (0.012)	P7	0.596 (0.001)	P7	0.521 (0.003)			T7	−0.364 (0.048)	C4	−0.399 (0.029)
	O1	0.436 (0.016)	P3	0.429 (0.018)					T8	−0.453 (0.012)		
			O1	0.412 (0.024)								
LPC→LMOG/ LCuneus	FP2	−0.481 (0.007)	FP1	−0.378 (0.039)	P7	0.416 (0.022)	T8	−0.397 (0.03)			C4	−0.509 (0.004)
	P7	0.417 (0.022)	FP2	−0.425 (0.019)							P8	−0.374 (0.042)
			T8	−0.367 (0.046)								
			P7	0.432 (0.017)								
LPC→LITG/LMTG	F7	−0.370 (0.044)	F7	−0.428 (0.018)	F7	−0.486 (0.006)	F7	−0.486 (0.006)	F8	−0.458 (0.011)	F8	−0.385 (0.036)
	P7	0.474 (0.008)	P7	0.502 (0.005)	P7	0.431 (0.017)	T7	−0.387 (0.035)			T7	−0.440 (0.015)
RMOG/ RCuneus→LITG/ LMTG											FP2	0.377 (0.040)
											F3	0.391 (0.033)
											F4	0.431 (0.017)
											P7	−0.370 (0.044)
RMOG/ RCuneus→LPH/ LFG	F3	0.389 (0.034)	P3	0.379 (0.039)			T8	−0.410 (0.025)	T8	−0.384 (0.036)	F7	0.389 (0.034)
LPC→RMOG/ RCuneus					Fz	0.364 (0.048)			T8	−0.408 (0.025)		

Note: *r(p)* is Correlation coefficients(probability); LPC, left Precuneus; LSFG/LMFG, left superior and middle frontal gyrus; LPH/LFG, left parahippocampal and fusiform gyrus; LMOG/LCuneus, left middle occipital gyrus and cuneus; LITG/LMTG, left inferior and middle temporal gyrus; RMOG/RCuneus, right middle occipital gyrus and cuneus.

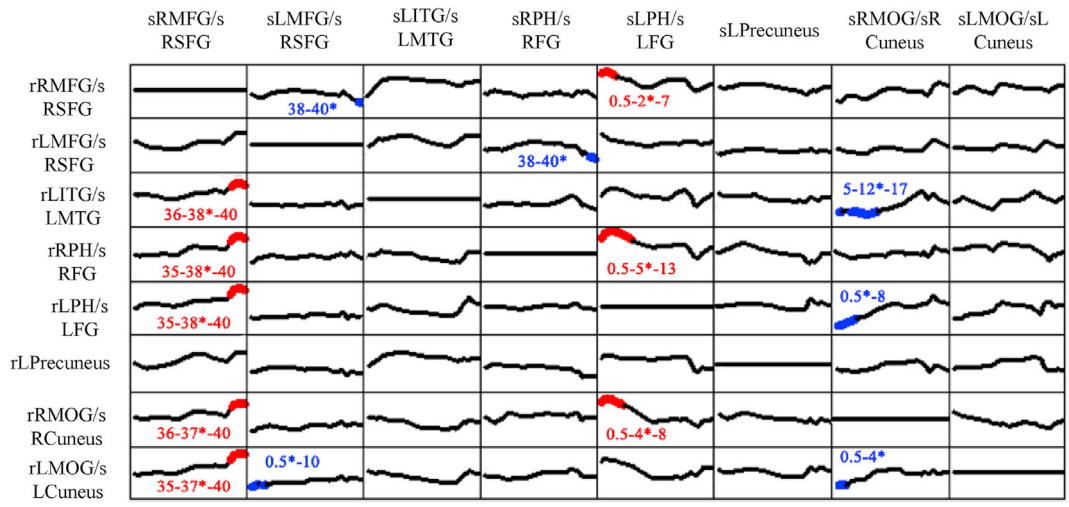

Fig. 5. Paired *t*-statistics comparing iCoh values after total sleep deprivation (TSD) and resting wakefulness in the resting-state task, in eight regions of interest: LSFG/LMFG, left superior and middle frontal gyrus, RSFG/RMFG, right superior and middle frontal gyrus, LITG/LMTG, left inferior and middle temporal gyrus, LPH/LFG, left parahippocampal and fusiform gyrus, RPH/RFG, right parahippocampal and fusiform gyrus, LMOG/LCuneus, left middle occipital gyrus and cuneus, RMOG/RCuneus, right middle occipital gyrus and cuneus. Frequency axis: 0.5–40 Hz. Corrected p = 0.05 at t-threshold = 2; vertical axis, −3.5 to +3.5. Blue color denotes stronger connectivity during RW compared with TSD; red color denotes stronger connectivity after TSD compared with RW. The three numbers in the figure represent the frequency (Hz) where significant results were obtained: the beginning, the most significant oscillation represented by the superscript "*", and the end. Columns are "sender" regions (prefix "s"), rows are "receiver" regions (prefix "r").

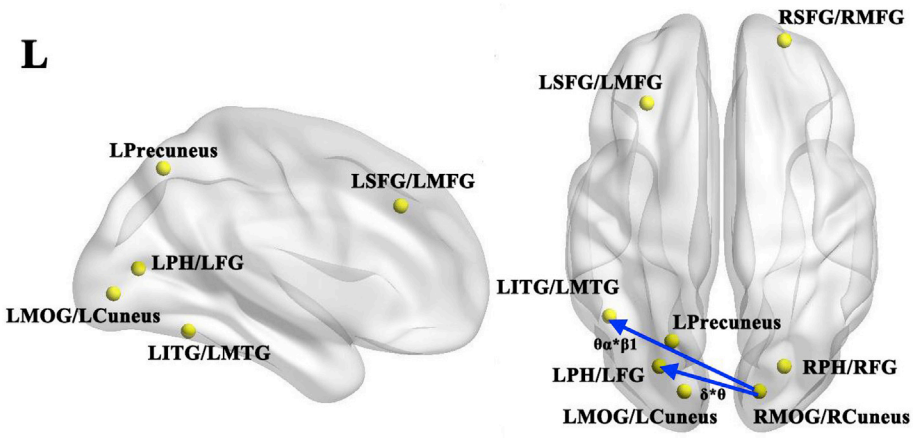

Fig. 6. Comparison of network properties between resting wakefulness and total sleep deprivation (TSD) in the resting-state task. Summary of the main statistically significant results. Blue color denotes stronger connectivity during RW compared with TSD; red color denotes stronger connectivity after TSD compared with RW. LSFG/LMFG, left superior and middle frontal gyrus; RSFG/RMFG, right superior and middle frontal gyrus; LITG/LMTG, left inferior and middle temporal gyrus; LPH/LFG, left parahippocampal and fusiform gyrus; RPH/RFG, right parahippocampal and fusiform gyrus; LMOG/LCuneus, left middle occipital gyrus and cuneus; RMOG/RCuneus, right middle occipital gyrus and cuneus. Frequency bands: δ, 0.5–4 Hz; θ, 4–7 Hz; α, 8–13 Hz; β1, 14–20 Hz; β2, 20–30 Hz; γ, 30–40 Hz.

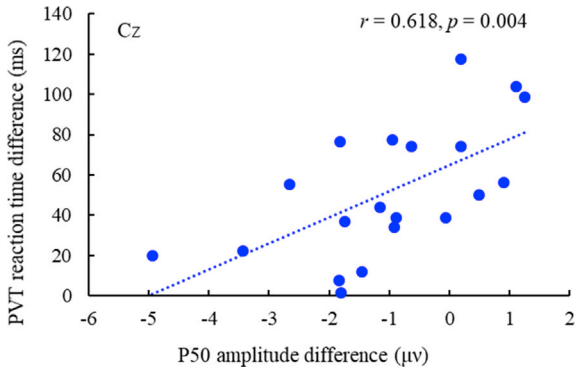

Fig. 7. Pearson correlation coefficient between P50 suppression and psychomotor vigilance task reaction time after total sleep deprivation (TSD) minus that at resting wakefulness (RW) at channel Cz ($r = 0.618$, $p = 0.004$).

component P50 amplitude values before and after sleep deprivation. We found that sleep deprivation impairs sensory gating. Specifically, alterations in P50 suppression positively correlated with changes in PVT reaction time, while disturbances in the effective connectivity among brain regions associated with the P50 task were found before and after TSD. TSD decreased the connectivity from the RMOG/RCuneus to the LITG/LMTG and LPH/FG, both during the resting-state and P50 tasks. Moreover, we found that the high-frequency oscillations from the precuneus to other brain regions (LSFG/LMFG, LITG/LMTG, LPH/LFG, LMOG/LCuneus) were strengthened during the P50 than during the resting-state task, indicating the impact of sleep deprivation on sensory gating. This is consistent with the left hemisphere P50 gating deficits observed in schizophrenia (Hanlon et al., 2005). Furthermore, correlations between changes in effective connectivity from the LPC to the LPH/LFG, LMOG/LCuneus, LITG/LMTG, and RMOG/RCuneus significantly negatively correlated with changes in the SG on the gamma band. These results indicate that the effective connectivity from the LPC to other brain regions is important for decreasing sensory gating after TSD. To our knowledge, our study is the first to employ effective connectivity to analyze the effects of sleep deprivation on sensory gating.

P50 suppression was significantly reduced after sleep deprivation. Moreover, changes in P50 suppression positively correlated with PVT changes. Further analysis showed that S2 amplitude increased, while S1 amplitude decreased, indicating that effective control of S2 by the brain is decreased after sleep deprivation. Consistently, Petrovsky et al. (2014) used PPI to study the effects of sleep deprivation on sensory gating and found that PPI markers were decreased. Several studies have shown that the allocation of attention resources changes after sleep deprivation (Alfarra et al., 2015; Lei et al., 2015; Massar et al., 2018). For example, Lei et al. (2015) found that salience networks allocate more attention resources to the default mode network to maintain alertness after TSD compared with RW. Although sensory gating is an adaptive strategy to save attention resources by reducing their allocation when re-encountering the same type of stimulus, this process seems to also involve higher cognitive function control (Krause et al., 2017). After sleep deprivation, an individual's sensory gating function is decreased, suggesting a deficit in higher control functions associated with cognitive resource allocation. The observed positive correlation between changes in P50 suppression and those in PVT reaction time before and after TSD suggest that this resource reallocation affects the individual's performance. These changes are expected to cause a greater wastage of the already reduced attention resources, further aggravating cognitive impairment in sleep-deprived individuals. As available attention resources decrease with longer sleep deprivation (Jin et al., 2015), this may result in P50 suppression.

Effective connectivity analysis of resting-state EEG data showed that sleep deprivation decreases the connection from the RMOG/RCuneus to the LITG/LMTG and LPH/LFG. The cuneus is mainly responsible for processing visual received information, while the temporal lobe is mainly responsible for processing auditory information (Crockford et al., 2005). The parahippocampal place area is a sub-region of the parahippocampal cortex that lies medially in the inferior temporo-occipital cortex and is important for the encoding and recognition of environmental scenes (rather than faces). Thus, the decline in these functional connections may be associated with an impairment in audiovisual information processing after sleep deprivation.

Effective connectivity analysis of P50-task EEG data confirmed that sleep deprivation decreases the connectivity from the RMOG/RCuneus to the LITG/LMTG and LPH/LFG, but also showed that it increased the high-frequency oscillations from the precuneus to the LITG/LMTG and LPH/LFG. The latter is more likely to be the mechanism underlying the changes in P50-task performance. Further correlation analysis indicated that, in the high frequency band, the increased effective connectivity between the LPC and LPH/LFG, LMOG/LCuneus, and LITG/LMTG before and after TSD negatively correlated with the change in P50 before and after sleep deprivation. These results also support the conclusion that effective connectivity from the LPC to other brain regions is important role for decreasing sensory gating after TSD. The precuneus is intimately associated with processing of individual feature information and has a different involvement when judging their familiarity, as it decides whether processing of perceptual features would be more useful (Boruchow, 1991). The LMTG, as an advanced center of auditory processing, is closely associated with processing of auditory information (Zaehle et al., 2004). In contrast, the FG and PH gyrus are both associated with neural pathways of identification (Calder and Young, 2005). Thus, increased effective connectivity between the precuneus and these regions (MTG, FG, and PH gyrus) after sleep deprivation reflects an increase in information exchange between the precuneus and temporal cortex,

indicating that the brain requires more cognitive resources to process auditory information after sleep deprivation. This could, in turn, lead to the decreased P50.

Previous studies have demonstrated enhanced activity in the prefrontal cortex when an individual completes a word task after sleep deprivation, which is believed to be a compensatory response by the brain for completing tasks (Drummond, 2000). We found that effective connectivity from the precuneus to the MFG was significantly higher after TSD compared with RW. However, there were no significant changes in the effective connectivity from the MFG to the precuneus and other brain regions, suggesting that the MFG might requires a higher information flow from the precuneus to maintain its function. This further implies that the brain needs to invest more energy to maintain sensory gating function under excessive mental fatigue. This may be a form of compensatory mechanism used by the brain to handle the negative effects of sleep deprivation.

There are several major limitations in this study. First, we did not control for circadian factors (time of the day), which have been shown to influence effective connectivity measures (Hodkinson et al., 2014). Thus, our results may indicate both the effects of circadian factors and of the 36-h TSD. Although we acquired the baseline data at 8 a.m., when subjects were well rested, it was hard to distinguish the effect of circadian factors from those of sustained wakefulness (36-h TSD). Second, the sample size was small, including only men, which may have affected the robustness of the results. Third, although subjects included in our analysis reported no sleep during the resting-state EEG recording, our results regarding the effective connectivity reduction under EEG monitoring need to be reproduced to exclude any intrusion of sleep. Fourth, during the PVT task, EEG analysis for micro-sleep would have been useful for ensuring that the subjects did not fall asleep, which should have been done in our research. Fifth, we only analyzed certain brain regions, but other regions may be involved in P50 suppression changes. However, we identified the related mechanism underlying the P50-suppression decline after TSD, which cannot be explained as a causal effect. In future studies, additional cognitive function tests should be performed, such as tests assessing the correlation between working memory, executive control, and effective connectivity changes before and after sleep deprivation, in order to further enrich the conclusions regarding the effects of sleep deprivation on cognition.

5. Conclusions

The current study used effective connectivity methods to examine how TSD impacts on brain sensory gating. We provide new evidence supporting a reduced integrity communication within sensory gating-related networks after TSD. Our results suggest that sleep deprivation could impair an individual's subconscious process.

Declaration of interest

None.

Acknowledgements

This research was funded by the National Military Science and Technology Commission Project [grant numbers 1716312ZT00210201], and the National Natural Science Foundation of China [grant numbers 81501622].

References

Adler, L.E., Pachtman, E., Franks, R.D., Pecevich, M., Waldo, M.C., Freedman, R., 1982. Neurophysiological evidence for a defect in neuronal mechanisms involved in sensory gating in schizophrenia. Biol. Psychiatry 17, 639–654. https://doi.org/10.1016/0920-9964(93)90048-N.

Alfarra, R., Fins, A.I., Chayo, I., Tartar, J.L., 2015. Changes in attention to an emotional task after sleep deprivation: neurophysiological and behavioral findings. Biol. Psychol. 104, 1–7. https://doi.org/10.1016/j.biopsycho.2014.11.001.

Anokhin, A.P., Vedeniapin, A.B., Heath, A.C., Korzyukov, O., Boutros, N.N., 2007. Genetic and environmental influences on sensory gating of mid-latency auditory evoked responses: a twin study. Schizophr. Res. 89, 312–319. https://doi.org/10.1016/j.schres.2006.08.009.

Bak, N., Glenthoj, B.Y., Rostrup, E., Larsson, H.B., Oranje, B., 2011. Source localization of sensory gating: a combined EEG and fMRI study in healthy volunteers. Neuroimage 54, 2711–2718. https://doi.org/10.1016/j.neuroimage.2010.11.039.

Boruchow, I.B., Hutchins, G.M., 1991. Delayed death from aortic root trauma. Ann. Thorac. Surg. 51, 317–319. https://doi.org/10.1016/0003-4975(91)90815-8.

Boutros, N.N., Belger, A., Campbell, D., D'Souza, C., Krystal, J., 1999. Comparison of four components of sensory gating in schizophrenia and normal subjects: a preliminary report. Psychiatr. Res. 88, 119–130. https://doi.org/10.1016/S0165-1781(99)00074-8.

Boutros, N.N., Korzyuko, O., Oliwa, G., Feingold, A., Campbell, D., McClain-Furmanski, D., Struve, F., Jansen, B.H., 2004. Morphological and latency abnormalities of the mid-latency auditory evoked responses in schizophrenia: a preliminary report. Schizophr. Res. 70, 303–313. https://doi.org/10.1016/j.schres.2003.12.009.

Braff, D.L., Light, G.A., 2004. Preattentional and attentional cognitive deficits as targets for treating schizophrenia. Psychopharmacology (Berlin) 174, 75–85. https://doi.org/10.1007/s00213-004-1848-0.

Bramon, E., Rabe-Hesketh, S., Sham, P., Murray, R.M., Frangou, S., 2004. Meta-analysis of the P300 and P50 waveforms in schizophrenia. Schizophr. Res. 70, 315–329. https://doi.org/10.1016/j.schres.2004.01.004.

Calder, A.J., Young, A.W., 2005. Understanding the recognition of facial identity and facial expression. Nat. Rev. Neurosci. 6, 641–651. https://doi.org/10.1038/nrn1724.

Chang, C., Leopold, D.A., Scholvinck, M.L., Mandelkow, H., Picchioni, D., Liu, X., Ye, F.Q., Turchi, J.N., Duyn, J.H., 2016. Tracking brain arousal fluctuations with fMRI. Proc. Natl. Acad. Sci. U. S. A. 113, 4518–4523.

Choo, W.C., Lee, W.W., Venkatraman, V., Sheu, F.S., Chee, M.W., 2005. Dissociation of cortical regions modulated by both working memory load and sleep deprivation and by sleep deprivation alone. Neuroimage 25, 579–587. https://doi.org/10.1016/j.neuroimage.2004.11.029.

Clementz, B.A., Blumenfeld, L.D., Cobb, S., 1997. The gamma band response may account for poor P50 suppression in schizophrenia. Neuroreport 8, 3889–3893. https://doi.org/10.1097/00001756-199712220-00010.

Cote, K.A., Milner, C.E., Osip, S.L., Baker, M.L., Cuthbert, B.P., 2008. Physiological arousal and attention during a week of continuous sleep restriction. Physiol. Behav. 95, 353–364. https://doi.org/10.1016/j.physbeh.2008.06.016.

Crockford, D.N., Goodyear, B., Edwards, J., Quickfall, J., el-Guebaly, N., 2005. Cue-induced brain activity in pathological gamblers. Biol. Psychiatry 58 (10), 787–795.

Deco, G., Corbetta, M., 2011. The dynamical balance of the brain at rest. Neuroscientist 17, 107–123.

Deco, G., Jirsa, V.K., McIntosh, A.R., 2011. Emerging concepts for the dynamical organization of resting-state activity in the brain. Nat. Rev. Neurosci. 12, 43–56.

de Gelder, B., Vroomen, J., Annen, L., Masthof, E., Hodiamont, P., 2003. Audio–visual integration in schizophrenia. Schizophr. Res. 59, 211–218. https://doi.org/10.1016/S0920-9964(01)00344-9.

Drummond, S.P., Brown, G.G., Gillin, J.C., Stricker, J.L., Wong, E.C., Buxton, R.B., 2000. Altered brain response to verbal learning following sleep deprivation. Nature 403, 655–657. https://doi.org/10.1038/35001068.

Freedman, R., Adler, L.E., Myles-Worsley, M., Nagamoto, H.T., Miller, C., Kisley, M., McRae, K., Cawthra, E., Waldo, M., 1996. Inhibitory gating of an evoked response to repeated auditory stimuli in schizophrenic and normal subjects: human recordings, computer simulation, and an animal model. Arch. Gen. Psychiatr. 53, 1114–1121. https://doi.org/10.1001/archpsyc.1996.01830120052009.

Freedman, R., Adler, L.E., Waldo, M.C., Pachtman, E., Franks, R.D., 1983. Neurophysiological evidence for a defect in inhibitory pathways in schizophrenia: comparison of medicated and drug-free patients. Biol. Psychiatry 18, 537–551.

Gumenyuk, V., Korzyukov, O., Roth, T., Bowyer, S.M., Drake, C.L., 2013. Sleep extension normalizes ERP of waking auditory sensory gating in healthy habitually short sleeping individuals. PLoS One 8, e59007. https://doi.org/10.1371/journal.pone.0059007.

Hamilton, H.K., Williams, T.J., Ventura, J., Jasperse, L.J., Owens, E.M., Miller, G.A., Subotnik, K.L., Nuechterlein, K.H., Yee, C.M., 2018. Clinical and cognitive significance of auditory sensory processing deficits in schizophrenia. Am. J. Psychiatry 175, 275–283. https://doi.org/10.1176/appi.ajp.2017.16111203.

Hanlon, F.M., Miller, G.A., Thoma, R.J., Irwin, J., Jones, A., Moses, S.N., Huang, M., Weisend, M.P., Paulson, K.M., Edgar, J.C., Adler, L.E., Cañive, J.M., 2005. Distinct M0 and M100 auditory gating deficits in schizophrenia. Psychophysiology 42, 417–427. https://doi.org/10.1111/j.1469-8986.2005.00299.x.

Havekes, R., Park, A.J., Tudor, J.C., Luczak, V.G., Hansen, R.T., Ferri, S.L., Bruinenberg, V.M., Poplawski, S.G., Day, J.P., Aton, S.J., Radwańska, K., Meerlo, P., Houslay, M.D., Baillie, G.S., Abel, T., 2016. Sleep deprivation causes memory deficits by negatively impacting neuronal connectivity in hippocampal area CA1. Elife 5, e13424. https://doi.org/10.7554/eLife.13424.

Hodkinson, D.J., O'Daly, O., Zunszain, P.A., Pariante, C.M., Lazurenko, V., Zelaya, F.O., Howard, M.A., Williams, S.C., 2014. Circadian and homeostatic modulation of functional connectivity and regional cerebral blood flow in humans under normal entrained conditions. J. Cereb. Blood Flow Metab. 34, 1493–1499. https://doi.org/10.1038/jcbfm.2014.109.

Jerger, K., Biggins, C., Fein, G., 1992. P50 suppression is not affected by attentional manipulations. Biol. Psychiatry 31, 365–377. https://doi.org/10.1016/0006-3223(92)90230-W.

Jin, X., Ye, E., Qi, J., Wang, L., Lei, Y., Chen, P., Mi, G., Zou, F., Shao, Y., Yang, Z., 2015. Recovery sleep reverses impaired response inhibition due to sleep restriction: evidence from a visual event related potentials study. PLoS One 10, e0142361. https://doi.org/10.1371/journal.pone.0142361.

Kenemans, J.L., Molenaar, P., Verbaten, M.N., Slangen, J.L., 1991. Removal of the ocular artifact from the EEG: a comparison of time and frequency domain methods with simulated and real data. Psychophysiology 28, 114–121. https://doi.org/10.1111/j.1469-8986.1991.tb03397.x.

Krause, A.J., Simon, E.B., Mander, B.A., Greer, S.M., Saletin, J.M., Goldstein-Piekarski, A.N., Walker, M.P., 2017. The sleep-deprived human brain. Nat. Rev. Neurosci. 18, 404–418. https://doi.org/10.1038/nrn.2017.55.

Lei, Y., Shao, Y., Wang, L., Zhai, T., Zou, F., Ye, E., Jin, X., Li, W., Qi, J., Yang, Z., 2015. Large-scale brain network coupling predicts total sleep deprivation effects on cognitive capacity. PLoS One 10, e0133959. https://doi.org/10.1371/journal.pone.0133959.

Lim, J., Dinges, D.F., 2010. Sleep deprivation and vigilant attention. Ann. N. Y. Acad. Sci. 1129, 305–322. https://doi.org/10.1196/annals.1417.002.

Massar, S.A.A., Lim, J., Sasmita, K., Chee, M.W.L., 2018. Sleep deprivation increases the costs of attentional effort: performance, preference and pupil size. Neuropsychologia 40, e213. https://doi.org/10.1016/j.neuropsychologia.2018.03.032.

Mayer, A.R., Hanlon, F.M., Franco, A.R., Teshiba, T.M., Thoma, R.J., Clark, V.P., Canive, J.M., 2009. The neural networks underlying auditory sensory gating. Neuroimage 44, 182–189. https://doi.org/10.1016/j.neuroimage.2008.08.025.

Monica, F., Low, K.A., Emily, W., Sable, J.J., Gabriele, G., 2006. Reduced suppression or labile memory? mechanisms of inefficient filtering of irrelevant information in older adults. J. Cogn. Neurosci. 18, 637–650. https://doi.org/10.1162/jocn.2006.18.4.637.

Morales-Muñoz, I., Jurado-Barba, R., Fernández-Guinea, S., Rodríguez-Jiménez, R., Jiménez-Arriero, M.A., Criado, J.R., Rubio, G., 2016. Sensory gating deficits in first-episode psychosis: evidence from neurophysiology, psychophysiology, and neuropsychology. J. Nerv. Ment. Dis. 204, 877–884. https://doi.org/10.1097/NMD.0000000000000572.

Nagamoto, H.T., Adler, L.E., Waldo, M.C., Freedman, R., 1989. Sensory gating in schizophrenics and normal controls: effects of changing stimulation interval. Biol. Psychiatry 25, 549–561. https://doi.org/10.1016/0006-3223(89)90215-1.

Nichols, T., Holmes, A.P., 2001. Nonparametric permutation tests for functional neuroimaging: a primer with examples. Hum. Brain Mapp. 15, 1–25.

Pascual-Marqui, R.D., 2007. Discrete, 3D Distributed, Linear Imaging Methods of Electric Neuronal Activity. Part 1: Exact, Zero Error Localization.

Pascual-Marqui, R.D., 2002. Standardized low-resolution brain electromagnetic tomography (sLORETA): technical details. Meth. Find. Exp. Clin. Pharmacol. 24, 5–12.

Pascual-Marqui, R.D., Biscay, R.J., Bosch-Bayard, J., Lehmann, D., Kochi, K., Yamada, N., Kinoshita, T., Sadato, N., 2014a. Isolated Effective Coherence (iCoh): Causal Information Flow Excluding Indirect Paths arXiv:1402.4887 [stat.ME].

Pascual-Marqui, R.D., Biscay, R.J., Bosch-Bayard, J., Lehmann, D., Kochi, K., Kinoshita, T., Yamada, N., Sadato, N., 2014b. Assessing direct paths of intracortical causal information flow of oscillatory activity with the isolated effective coherence (iCoh). Front. Hum. Neurosci. 8, 1–12. https://doi.org/10.3389/fnhum.2014.00448.

Pascual-Marqui, R.D., Lehmann, D., Koukkou, M., Kochi, K., Anderer, P., Saletu, B., Tanaka, H., Hirata, K., John, E.R., Prichep, L., Biscay-Lirio, R., Kinoshita, T., 2011. Assessing interactions in the brain with exact low-resolution electromagnetic tomography. Philos. Trans. A Math. Phys. Eng. Sci. 369, 3768–3784. https://doi.org/10.1098/rsta.2011.0081.

Petrovsky, N., Ettinger, U., Hill, A., Frenzel, L., Meyhöfer, I., Wagner, M., Backhaus, J., Kumari, V., 2014. Sleep deprivation disrupts prepulse inhibition and induces psychosis-like symptoms in healthy humans. J. Neurosci. 34, 9134–9140. https://doi.org/10.1523/JNEUROSCI.0904-14.2014.

Piantoni, G., Cheung, B.L., Van Veen, B.D., Romeijn, N., Riedner, B.A., Tononi, G., Van Der Werf, Y.D., Van Someren, E.J., 2013. Disrupted directed connectivity along the cingulate cortex determines vigilance after sleep deprivation. Neuroimage 79, 213–222. https://doi.org/10.1016/j.neuroimage.2013.04.103.

Pizzagalli, D.A., Oakes, T.R., Fox, A.S., Chung, M.K., Larson, C.L., Abercrombie, H.C., Schaefer, S.M., Benca, R.M., Davidson, R.J., 2004. Functional but not structural subgenual prefrontal cortex abnormalities in melancholia. Mol. Psychiatr. 9, 393–340. https://doi.org/10.1038/sj.mp.4001469.

Price, E., Moore, G., Galway, L., Linden, M., 2017. Validation of a smartphone-based approach to in situ cognitive fatigue assessment. JMIR Mhealth Uhealth 5, e125. https://doi.org/10.2196/mhealth.6333.

Ridder, D.D., Congedo, M., Vanneste, S., 2015. The neural correlates of subjectively perceived and passively matched loudness perception in auditory phantom perception. Brain Behav. 5 (5), e00331, 2015. https://doi.org/10.1002/brb3.331.

Ringel, T.M., Heidrich, A., Jacob, C.P., Pfuhlmann, B., Stoeber, G., Fallgatter, A.J., 2004. Sensory gating deficit in a subtype of chronic schizophrenic patients. Psychiatry 125, 237–245. https://doi.org/10.1016/j.psychres.2004.01.004.

Rosenberg, M.D., Finn, E.S., Scheinost, D., Papademetris, X., Shen, X., Constable, R.T., Chun, M.M., 2016. A neuromarker of sustained attention from whole-brain functional connectivity. Nat. Neurosci. 19, 165–171.

Ross, L.A., Saint-Amour, D., Leavitt, V.M., Molholm, S., Javitt, D.C., Foxe, J.J., 2007. Impaired multisensory processing in schizophrenia: deficits in the visual enhancement of speech comprehension under noisy environmental conditions. Schizophr. Res. 97, 173–183. https://doi.org/10.1016/j.schres.2007.08.008.

Tregellas, J.R., Davalos, D.B., Rojas, D.C., Waldo, M.C., Gibson, L., Wylie, K., Du, Y.P., Freedman, R., 2007. Increased hemodynamic response in the hippocampus, thalamus and prefrontal cortex during abnormal sensory gating in schizophrenia. Schizophr. Res. 92, 262–272. https://doi.org/10.1016/j.schres.2006.12.033.

Verweij, I.M., Romeijn, N., Smit, D.J., Piantoni, G., Van Someren, E.J., van der Werf, Y.D., 2014. Sleep deprivation leads to a loss of functional connectivity in frontal brain regions. BMC Neurosci. 15, 88. https://doi.org/10.1186/1471-2202-15-88.

Wagner, M., Fuchs, M., Kastner, J., 2004. Evaluation of sLORETA in the presence of noise and multiple sources. Brain Topogr. 16, 277–280. https://doi.org/10.1023/B:BRAT.0000032865.58382.62.

Wang, C., Ong, J.L., Patanaik, A., Zhou, J., Chee, M.W., 2016. Spontaneous eyelid closures link vigilance fluctuation with fMRI dynamic connectivity states. Proc. Natl. Acad. Sci. U. S. A. 113, 9653–9658.

Wu, X., Chen, J., Yang, L., Ma, W., Jia, T., Hua, Z., Wu, Y., 2013. Effects of 36 h sleep deprivation on P50 auditory sensory gating potential in young soldiers. J. Shanxi. Med. Univ. 44, 200–202. https://doi.org/10.3969/J.ISSN.1007-6611.2013.03.009.

Zaehle, T., Wüstenberg, T., Meyer, M., Jäncke, M., 2004. Evidence for rapid auditory perception as the foundation of speech processing: a sparse temporal sampling fMRI study. Eur. J. Neurosci. 20, 2447–2456. https://doi.org/10.1111/j.1460-9568.2004.03687.x.

Zumsteg, D., Lozano, A.M., Wennberg, R.A., 2006a. Mesial temporal inhibition in a patient with deep brain stimulation of the anterior thalamus for epilepsy. Epilepsia 47, 1958–1962. https://doi.org/10.1111/j.1528-1167.2006.00824.x.

Zumsteg, D., Lozano, A.M., Wennberg, R.A., 2006b. Depth electrode recorded cerebral responses with deep brain stimulation of the anterior thalamus for epilepsy. Clin. Neurophysiol. 117, 1602–1609.